

Manuscript Number:

Title: Anisotropy of piezocaloric effect at ferroelectric phase transitions in ammonium hydrogen sulphate

Article Type: Full Length Article

Keywords: piezocaloric effect, phase transition, ferroelectrics, thermal expansion, high-pressure, entropy

Corresponding Author: Professor Igor Flerov,

Corresponding Author's Institution: Kirensky Institute of Physics

First Author: Igor Flerov

Order of Authors: Igor Flerov; Ekaterina Mikhaleva; Mikhail Gorev; Maxim Molocheev; Andrey Kartashev

Abstract: The role of anisotropy of the thermal expansion in formation of piezocaloric effect (PCE) near ferroelectric phase transitions in  $\text{NH}_4\text{HSO}_4$  was studied. Strong difference in linear baric coefficients and as a result in intensive and extensive PCE associated with the different crystallographic axes was found. PCE giving the main contribution to the barocaloric effect were determined at both phase transitions. Rather strong effect of the lattice dilatation on the tuning of PCE was observed. Comparative analysis of PCE at the phase transitions in different materials showed that  $\text{NH}_4\text{HSO}_4$  can be considered as a promising solid-state refrigerant. A hypothetical cooling cycle based on alternate using uniaxial pressure along two axes was considered.

Dear Editor,

Consider please our manuscript, devoted to pioneering studies of the intensive and extensive piezocaloric effects near phase transitions in ferroelectric  $\text{NH}_4\text{HSO}_4$ .

We hope that the results will be of interest to readers of Journal of Alloys and Compounds.

Sincerely Yours,

Prof. Igor Flerov

## **Anisotropy of piezocaloric effect at ferroelectric phase transitions in ammonium hydrogen sulphate**

Ekaterina A. Mikhaleva, Mikhail V. Gorev, Maxim S. Molokeev, Andrey V. Kartashev, Igor N. Flerov

e-mail: [katerina@iph.krasn.ru](mailto:katerina@iph.krasn.ru) (E.A. Mikhaleva), [gorev@iph.krasn.ru](mailto:gorev@iph.krasn.ru) (M.V. Gorev), [msmolokeev@mail.ru](mailto:msmolokeev@mail.ru) (M.S/ Molokeev), [avkartashev@yandex.ru](mailto:avkartashev@yandex.ru) (A.V. Kartashev), [flerov@iph.krasn.ru](mailto:flerov@iph.krasn.ru) (I.N. Flerov),

### **Abstract**

The role of anisotropy of the thermal expansion in formation of piezocaloric effect (PCE) near ferroelectric phase transitions in  $\text{NH}_4\text{HSO}_4$  was studied. Strong difference in linear baric coefficients and as a result in intensive and extensive PCE associated with the different crystallographic axes was found. PCE giving the main contribution to the barocaloric effect were determined at both phase transitions. Rather strong effect of the lattice dilatation on the tuning of PCE was observed. Comparative analysis of PCE at the phase transitions in different materials showed that  $\text{NH}_4\text{HSO}_4$  can be considered as a promising solid-state refrigerant. A hypothetical cooling cycle based on alternate using uniaxial pressure along two axes was considered.

### Prime Novelty Statement

- 1) Pioneering studies of the role of anisotropy of crystal lattice in formation of the piezocaloric properties in a ferroelectric material are performed
- 2) Ammonium hydrogen sulphate,  $\text{NH}_4\text{HSO}_4$ , undergoing a succession of two phase transitions,  $\text{P}2_1/c(\text{T}_1) \leftrightarrow \text{P}c(\text{T}_2) \leftrightarrow \text{P}1$ , was chosen as model object due to large difference in origin, type and sensitivity to external pressure of structural transformations.
- 3) A strong anisotropy of thermal expansion in the region of both phase transitions leads to a significant difference in the signs and values of linear baric coefficients.
- 4) The greatest magnitudes of piezocaloric effect at  $\text{T}_1$  and  $\text{T}_2$  are related to different axes and provide the main contribution to the barocaloric effect, considered as the sum of linear effects.
- 5) A strong nonlinearity of the dependences of the intensive and extensive piezocaloric effects at the first order transformation  $\text{P}c \leftrightarrow \text{P}1$  leads to low mechanical stresses to achieve the maximum possible values of both effects.
- 6) Taking into account the thermal expansion of the crystal lattice, the greatest changes in piezocaloric effect is found at  $\text{T}_1$ .
- 7)  $\text{NH}_4\text{HSO}_4$  can be considered as competitive solid refrigerant in comparison with other materials. Due to strong anisotropy of piezocaloric effect at  $\text{T}_2$ , thermodynamic efficiency of the cooling cycle can be improved by alternate using uniaxial pressure along axes  $a$  and  $c$ .
- 5) The results obtained are very important and promising in terms of the possibility of increasing the caloric efficiency of solid-state refrigerants.

# Anisotropy of piezocaloric effect at ferroelectric phase transitions in ammonium hydrogen sulphate

Ekaterina A. Mikhaleva<sup>a</sup>, Mikhail V. Gorev<sup>a,b</sup>, Maxim S. Molokeev<sup>a,b,c</sup>,  
Andrey V. Kartashev<sup>a,d</sup>, Igor N. Flerov<sup>a,b,\*</sup>

<sup>a</sup>*Kirensky Institute of Physics, Federal Research Center KSC SB RAS, 660036  
Krasnoyarsk, Russia*

<sup>b</sup>*Institute of Engineering Physics and Radioelectronics, Siberian Federal University, 660074  
Krasnoyarsk, Russia*

<sup>c</sup>*Department of Physics, Far Eastern State Transport University, 680021 Khabarovsk,  
Russia*

<sup>d</sup>*Astafjev Krasnoyarsk State Pedagogical University, 660049 Krasnoyarsk, Russia*

---

## Abstract

The role of anisotropy of the thermal expansion in formation of piezocaloric effect (PCE) near ferroelectric phase transitions in  $\text{NH}_4\text{HSO}_4$  was studied. Strong difference in linear baric coefficients and as a result in intensive and extensive PCE associated with the different crystallographic axes was found. PCE giving the main contribution to the barocaloric effect were determined at both phase transitions. Rather strong effect of the lattice dilatation on the tuning of PCE was observed. Comparative analysis of PCE at the phase transitions in different materials showed that  $\text{NH}_4\text{HSO}_4$  can be considered as a promising solid-state refrigerant. A hypothetical cooling cycle based on alternate using uniaxial pressure along two axes was considered.

*Keywords:* piezocaloric effect, phase transition, ferroelectrics, thermal expansion, high-pressure, entropy

*PACS:* 62.50.-p, 64.70.K-, 65.40.-b, 65.40.De

---

\*Corresponding author

*Email addresses:* [katerina@iph.krasn.ru](mailto:katerina@iph.krasn.ru) (Ekaterina A. Mikhaleva),  
[gorev@iph.krasn.ru](mailto:gorev@iph.krasn.ru) (Mikhail V. Gorev), [mamolokeev@mail.ru](mailto:mamolokeev@mail.ru) (Maxim S. Molokeev),  
[akartashev@yandex.ru](mailto:akartashev@yandex.ru) (Andrey V. Kartashev), [flerov@iph.krasn.ru](mailto:flerov@iph.krasn.ru) (Igor N. Flerov)

## 1. Introduction

Solids exhibiting high caloric effects (CE) attract a great attention of both researches and engineers due a possibility to use them as effective solid-state refrigerants at designing alternative cooling cycles[1, 2, 3, 4, 5]. Different CE exist according to their physical nature: magnetocaloric (MCE), electrocaloric (ECE), barocaloric (BCE), piezo-(or elasto-)caloric PCE(EICE), flexocaloric (FCE). All these effects are associated with a reversible change in the adiabatic temperature ( $\Delta T_{AD}$ ) or isothermal entropy ( $\Delta S_{CE}$ ) of the material when the corresponding external field is applied or removed.

Studies of caloric materials are mainly carried out in two directions. The former is related to the search for solids competitive in caloric efficiency relative to gas coolants used in traditional large-scale gas-compressor refrigerators. In such a case, materials with significant intensive,  $\Delta T_{AD}$ , and extensive,  $\Delta S_{CE}$ , MCE and BCE look like the most promising [2, 6, 7].

The main objective of the latter direction is to create solid refrigerants that can be used in miniature refrigerators, essential for modern micro- and nano-electronic devices with large heat emission [8]. Obviously, for this purpose, the most suitable are crystalline or ceramic dielectric materials that do not require bulky external devices for the implementation of individual or pairing CE: ECE, PCE (EICE), FCE. The disadvantages of ECE and FCE are associated, first, with the irreversible process of Joule heat generation in a ferroelectric when high electric field is applied and, second, with a significant nonlinear deformation of the caloric element which is not very convenient, for example, when designing combined working elements of the microcircuit-refrigerator.

PCE can be considered as a special case of the bulk BCE, coupled with hydrostatic pressure, and is realized under the influence of uniaxial mechanical stress  $\sigma$ :

$$\Delta S_{PCE} = - \int V_m(T, \sigma) \alpha(T, \sigma) d\sigma; \quad \Delta T_{AD}^{PCE} = - \frac{T}{C_p} \Delta S_{PCE}, \quad (1)$$

where  $V_m$  is the molar volume and  $\alpha = l^{-1}(\partial l / \partial T)_\sigma$  is a linear thermal expansion coefficient.

For the first time experimental studies of PCE were carried out by Joule in the 19<sup>th</sup> century [9]. He performed the measurements at room temperature and found that the response of the temperature of the samples under stress depends  
30 on the type of material (wood, metals. etc.) as well as the magnitude of the tensile/compressive load and is rather small, mainly due to the small values of the coefficient  $\alpha$  of the materials studied.

It is known, however, that thermal expansion can significantly increase in the region of phase transition of various physical origin. The reason is that linear/volume strain either is itself an order parameter (ferroelastic and martensitic transformations) or is strongly related to the principal order parameter of  
35 a different nature (magnetization, polarization). In both cases, a pronounced anomalous behavior of the coefficient  $\alpha$  is observed in the vicinity of the transition point.

In recent years, much attention has been paid to the study of PCE in  
40 shape memory alloys undergoing the martensitic transformations accompanied by large entropy change [10, 11, 12, 13]. Rather low tensile and compressive stresses created in the samples in the form of wire or ribbon led to significant values of  $\Delta T_{AD}$  and  $\Delta S_{CE}$  in some materials [14, 15].

However, in the case of alloys, PCE was measured only in one direction.  
45 On the other hand, as can be seen from Eq. 1, it is obvious that in anisotropic materials, the magnitude and sign of PCE can be different in accordance with the difference in the coefficients along different directions. Recently, we have proved this assumption studying PCE near ferroelastic phase transitions in some orthorhombic single crystals [16, 17]. It was found that anisotropy of the crystal  
50 lattice allows one to realize conventional ( $\Delta T_{AD} > 0$ ,  $\Delta S_{CE} < 0$ ) and inverse ( $\Delta T_{AD} < 0$ ,  $\Delta S_{CE} > 0$ ) PCE in the same sample using uniaxial stresses applying along different crystallographic axes. We have also demonstrated that in some case the values of the uniaxial CE can be comparable with BCE or even  
55 exceed it.

PCE in some ferroelectrics (ceramics, films and single crystals) was studied experimentally and in the scope of some theoretical approaches only to a small

extent [18, 19, 20, 21]. Moreover, in these materials the effect was also considered only for one direction in the sample and never the attention was paid to the  
60 anisotropy of PCE.

Analysis performed recently by U.S. Department of Energy showed that studies of thermoelastic effects (PCE and BCE) in solids are the most promising in terms of the development of alternative cooling technologies [22].

In the present paper, we analyzed the effect of anisotropy of thermal ex-  
65 pansion on the intensive and extensive piezocaloric efficiency of ferroelectric  $\text{NH}_4\text{HSO}_4$  using method developed by us earlier [16, 17]. Ammonium hydrogen sulphate was chosen as very convenient model object due to its peculiar and interesting properties. Firstly, it undergoes the succession of two phase transitions  $P2_1/c (T_1=271 \text{ K}) \leftrightarrow Pc (T_2=159 \text{ K}) \leftrightarrow P1$ , of the second and first  
70 order, respectively, which are far rather from the tricritical point [23]. Secondly, these transformations also differ greatly from each other by entropy parameters ( $\Delta S_1=1.2 \text{ J/mol}\cdot\text{K}$ ,  $\Delta S_2=6.7 \text{ J/mol}\cdot\text{K}$ ) and sensitivity to hydrostatic pressure ( $dT_1/dp=+90\pm 15 \text{ K/GPa}$  and  $dT_2/dp=-123\pm 15 \text{ K/GPa}$ ). Thirdly, strong effect of the hydrostatic pressure on the entropy jump associated with the first  
75 order phase transition at  $T_2$  was observed but information on the temperature hysteresis was absent. Fourthly, far from the phase transition points,  $\text{NH}_4\text{HSO}_4$  is characterized by rather large coefficient of the volume thermal expansion of the crystal lattice,  $\beta_{LAT}=(1.5-2.0)\cdot 10^{-4} \text{ K}^{-1}$ . In accordance with [24], this can significantly effects on BCE. However, the question of the influence of thermal  
80 expansion of the crystal lattice on PCE in ferroelectrics remained open.

Taking in mind the points above, we performed detailed experimental study of linear thermal expansion near both phase transition in  $\text{NH}_4\text{HSO}_4$  as well as hysteretic phenomena around  $T_2$ .

## 2. Experimental

85 Rather large single crystals of  $\text{NH}_4\text{HSO}_4$  were grown by slow evaporation at  $45^\circ\text{C}$  from aqueous solution containing equimolar quantities of  $(\text{NH}_4)_2\text{SO}_4$  and

H<sub>2</sub>SO<sub>4</sub>.

XRD examination of the quality of the sample at room temperature was performed with a Bruker D8 ADVANCE powder diffractometer (Cu-K $\alpha$  radiation), TTK 450 Anton Paar heat attachment and linear VANTEC detector. It revealed, firstly, a monoclinic symmetry (sp. gr.  $P2_1/c$ ,  $Z=8$ ), consistent with suggested in [23, 25, 26] and, secondly, the absence of any additional phases. Fig. 1 shows the results of Rietveld refinement ( $R_{wp}=6.04$ ,  $R_p=4.23$ ,  $\chi^2=2.06$ ).

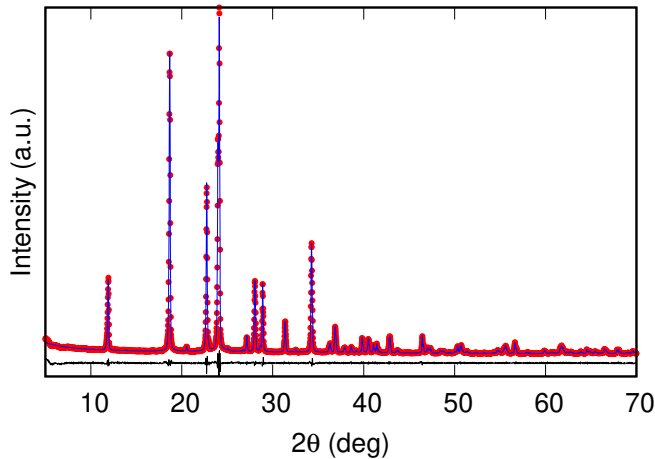


Figure 1: Difference Rietveld plot for NH<sub>4</sub>HSO<sub>4</sub> at room temperature.

A good agreement was found between the unit cell parameters in the sample under study ( $a=14.3954(7)\text{\AA}$ ,  $b=4.5938(2)\text{\AA}$ ,  $c=14.8343(8)\text{\AA}$ ,  $\beta=120.883(2)$  grad) and those determined earlier in [25, 26].

Further experimental procedure was organized taking in mind the peculiarities of the phase transitions in NH<sub>4</sub>HSO<sub>4</sub>, Due to a large volume change in the region of the first order phase transition  $Pc \leftrightarrow P1$ , detected when measuring on quasi-ceramic samples prepared using the solution and melt technology [23], we assumed that single-crystal samples may crack during experiments with heat treatments around  $T_2$ .

Therefore, experimental studies were carried out in several stages. At the first stage, the behavior of linear thermal expansion was studied on single-crystal



specimen in the range from 175 K to 320 K including the vicinity of the second order phase transition  $P2_1/c \leftrightarrow Pc$ . The  $\text{NH}_4\text{HSO}_4$  sample was cut in the form of rectangular prism with the dimensions of  $7.4 \times 8.6 \times 5.9 \text{ mm}^3$  along crystallographic axes  $a$ ,  $b$ ,  $c$  for the pseudo-orthorhombic cell. Measurements were performed in a vacuum atmosphere ( $\sim 10^{-2} \text{ mm Hg}$ ) using a quartz optic-  
 110 mechanical dilatometer with a sensitivity of  $1.2 \times 10^{-6} \text{ cm}$ . Temperature step of discrete heating was  $\leq 0.5 \text{ K}$  and  $\geq 2 \text{ K}$  near and far from  $T_1$ , respectively.

At the second stage, the same sample was examined using an a homemade adiabatic calorimeter [27] in continuous cooling/heating mode through the phase transition  $Pc \leftrightarrow P1$  at a very low temperature variation rate of about  $dT/dt =$   
 115  $\pm 10^{-3} \text{ K/min}$ . It was found that, indeed, single-crystal sample was cracked after cooling/heating through the phase transition  $Pc \leftrightarrow P1$ . Thus, we were unable to measure the linear expansion of the  $\text{NH}_4\text{HSO}_4$  single-crystal around  $T_2$  using a quartz dilatometer.

Therefore, at the next stage, X-ray studies were performed on a powder sam-  
 120 ple to get information on the temperature behavior of the unit cell parameters. Measurements were carried out in the temperature range from 155 K to 180 K with the step of about 1 K.

### 3. Results and Discussion

First of all it is worth to discuss the hysteretic phenomena observed in calori-  
 125 metric experiments near  $T_2$ . The hysteresis of the phase transition temperature was found of about  $\delta T_2 = 2.5 \text{ K}$ . The entropy jump  $\delta S_2$  decreases with pressure increase and is equal to zero at rather low pressure of the tricritical point  $p_{tcp} \approx 0.18 \pm 0.02 \text{ GPa}$  [23]. The rapid approach of the phase transition under pressure to the tricritical point accompanied by  $\delta T_2 \rightarrow 0$  is an important prop-  
 130 erty of  $\text{NH}_4\text{HSO}_4$  and can be considered as very useful for the implementation of a reliable and stable BCE and PCE [3].

The temperature dependencies of the linear thermal expansion coefficients,  $\alpha_i$ , in the vicinity  $T_1$  and unit cell parameters,  $a_i$ , around  $T_2$  are shown in Fig. 2

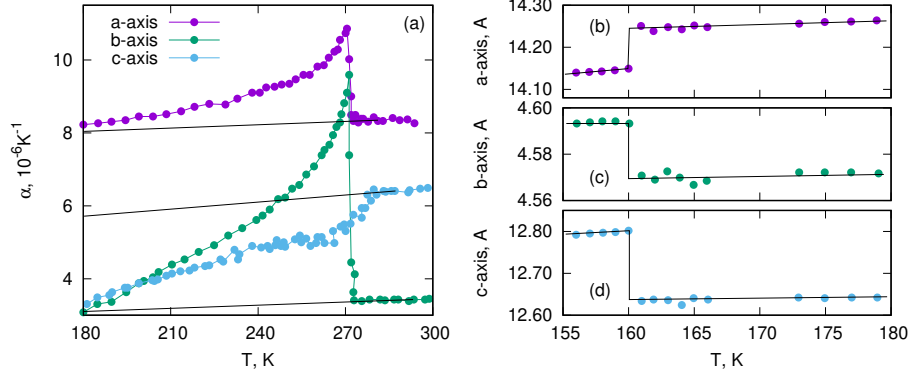


Figure 2: Temperature dependencies of (a) thermal expansion coefficients  $\alpha_i$  near  $T_1$  and (b,c,d) cell parameters  $a$ ,  $b$  and  $c$  for the pseudo-orthorhombic cell near  $T_2$  in  $\text{NH}_4\text{HSO}_4$ .

(a) and (b). X-ray data are also presented for the pseudo-orthorhombic cell. It  
 135 can be seen that far from the phase transition points,  $\text{NH}_4\text{HSO}_4$  is characterized  
 by a positive thermal dilatation in all crystallographic directions. The values  
 of  $\alpha_i$  evaluated at 180 K from dependencies of  $\alpha_i(T)$  ( $\alpha_a = +(7.5 \pm 0.8) \cdot 10^{-5}$   
 $\text{K}^{-1}$ ;  $\alpha_b = +(3.5 \pm 0.5) \cdot 10^{-5} \text{K}^{-1}$ ;  $\alpha_c = +(6.4 \pm 0.7) \cdot 10^{-5} \text{K}^{-1}$ ) agree well  
 with coefficients determined in dilatometric experiments (Fig. 2(a)).

140 A highly anisotropic anomalous behavior of thermal expansion was found at  
 both  $T_1$  and  $T_2$ . The jumps at the phase transition points of the linear expansion  
 coefficients,  $\delta\alpha_i = \alpha_i - \alpha_i^{LAT}$  ( $\alpha_i^{LAT}$  is a lattice contribution), and linear strains,  
 $\delta(\Delta\alpha_i/a_i) = (\Delta\alpha_i/a_i)_{T>T_2} - (\Delta\alpha_i/a_i)_{T<T_2}$ , are presented in Table 1.

Different signs of  $\delta\alpha_i$  and  $\delta(\Delta a_i/a_i)$  values associated with different axes  
 145 indicate that in accordance with Eq. 1, PCE can be realized as conventional or  
 inverse. Summation of the jumps of the unit cell parameters,  $\sum \delta(\Delta a_i/a_i) =$   
 $\delta(\Delta V/V)$ , and linear expansion coefficients,  $\sum \delta\alpha_i = \delta\beta$ , show that jumps in  
 volume strain and coefficient  $\beta$  have different signs and this determines the  
 difference of signs of baric coefficients for the phase transitions in ammonium  
 150 hydrogen sulphate ( $dT_1/dp=90 \text{ K/GPa}$ ;  $dT_2/dp=-123 \text{ K/GPa}$ ) [23].

Sensitivity of the phase transition temperatures in  $\text{NH}_4\text{HSO}_4$  to uniaxial  
 stress,  $dT_1/d\sigma_i$  and  $dT_2/d\sigma_i$ , was determined in the scope of the Ehrenfest,

Table 1: Some parameters of the thermal expansion at the phase transition points  $T_1$  and  $T_2$  in  $\text{NH}_4\text{HSO}_4$ .  $\delta\alpha_i$  and  $\delta\beta$  – jumps of the linear and volume expansion coefficients.  $\delta a_i/a_i$  and  $\delta V/V$  – jumps of parameters and volume of the unit cell.  $dT/d\sigma_i$  and  $(dT/dp)$  – shift of the phase transition temperatures under uniaxial and hydrostatic pressure.

	$P2_1/c \leftrightarrow Pc$	$Pc \leftrightarrow P1$	Ref.
$\delta\alpha_a \cdot 10^6, \text{K}^{-1}$	$+(25.5 \pm 1.0)$		
$\delta\alpha_b \cdot 10^6, \text{K}^{-1}$	$+(64.5 \pm 3.0)$		
$\delta\alpha_c \cdot 10^6, \text{K}^{-1}$	$-(8.0 \pm 0.5)$		
$\delta\beta \cdot 10^6, \text{K}^{-1}$	$+(82.0 \pm 4.5)$		
$\delta a/a, \%$		$+(0.69 \pm 0.03)$	
$\delta b/b, \%$		$-(0.52 \pm 0.02)$	
$\delta c/c, \%$		$-(1.27 \pm 0.06)$	
$\delta V/V, \%$		$-(1.10 \pm 0.11)$	
$dT_1/d\sigma_a, \text{K} \cdot \text{GPa}^{-1}$	$+(33 \pm 5)$		
$dT_1/d\sigma_b, \text{K} \cdot \text{GPa}^{-1}$	$+(79 \pm 10)$		
$dT_1/d\sigma_c, \text{K} \cdot \text{GPa}^{-1}$	$-(10 \pm 3)$		
$(dT_1/dp)_{calc}, \text{K} \cdot \text{GPa}^{-1}$	$+(102 \pm 18)$		
$(dT_1/dp)_{exp}, \text{K} \cdot \text{GPa}^{-1}$	$+(90 \pm 15)$		[23]
$dT_2/d\sigma_a, \text{K} \cdot \text{GPa}^{-1}$		$+(45 \pm 4)$	
$dT_2/d\sigma_b, \text{K} \cdot \text{GPa}^{-1}$		$-(50 \pm 5)$	
$dT_2/d\sigma_c, \text{K} \cdot \text{GPa}^{-1}$		$-(122 \pm 7)$	
$(dT_2/dp)_{calc}, \text{K} \cdot \text{GPa}^{-1}$		$+(127 \pm 16)$	
$(dT_2/dp)_{exp}, \text{K} \cdot \text{GPa}^{-1}$		$-(123 \pm 15)$	[23]

$dT_1/d\sigma_i = T \cdot \delta\alpha_i/\delta C_p$ , and Clapeyron–Clausius,  $dT_2/d\sigma_i = \delta(\Delta a_i/a_i)/\delta S$ , re-  
 lations using data on the jumps in entropy  $\delta S$ , heat capacity  $\delta C_p$  [23], linear  
 155 strain  $\delta(\Delta a_i/a_i)$  and coefficient of the linear thermal expansion  $\delta(\Delta\alpha_i)$ . The  
 results of calculations are presented in (Table 1). It is evident that in accordance  
 with the strong anisotropy of the thermal dilatation there is a large difference  
 in the values and signs of the coefficients  $dT/d\sigma_i$ . Table 1 also demonstrates  
 that the largest values of  $dT/d\sigma_i$  at  $T_1$  and  $T_2$  are, firstly, related to different  
 160 crystallographic axes, and secondly, they are the largest contributors to the  
 $dT_1/dp$  and  $dT_2/dp$  values. The reliability of the data obtained is confirmed by  
 a good agreement of the calculated,  $(dT/dp)_{calc}$  and experimentally determined  
 $(dT/dp)_{exp}$  baric coefficients (Table 1).

In order to determine the intensive and extensive PCE in  $\text{NH}_4\text{HSO}_4$ , we  
 165 used previously obtained results of the separation of the anomalous,  $\Delta S_1(T)$   
 and  $\Delta S_2(T)$ , and lattice,  $S_{LAT}$ , entropies at  $p = 0$  [23]. It was mentioned above  
 that at  $p \approx 0.2$  GPa the phase transition at  $T_2$  exhibits a tricritical behavior  
 with  $\delta S_2 = 0$ . However, it is unlikely that such a low pressure can change the  
 degree of disordering of structural elements in the initial phase, and, as a result,  
 170 the magnitudes of total excess entropies  $\Delta S_1$  and  $\Delta S_2$  can be considered as  
 unchanged.

The total entropy as a function of temperature,  $S(T)$ , at different  $\sigma_i > 0$   
 was determined by summation of  $S_{LAT}$  and anomalous contributions  $\Delta S_1(T)$   
 as well as  $\Delta S_2(T)$  at  $\sigma_i = 0$  shifted along the temperature scale according to  
 the values of  $dT_1/d\sigma_i$  and  $dT_2/d\sigma_i$ .

$$S(T, \sigma_i) = S_{LAT}(T) + \Delta S_1(T + (dT_1/d\sigma_i)\sigma_i) + \Delta S_2(T + (dT_2/d\sigma_i)\sigma_i) \quad (2)$$

It should be noted that this procedure was carried out at two different  
 conditions: first, without taking into account, and second, taking into ac-  
 count the thermal expansion of the crystal lattice. In the latter case, the  
 175 lattice entropy change under pressure was determined using Maxwell relation

$$(\partial S_{LAT}/\partial \sigma_i)_T = (\partial(\Delta a_i/a_i)/\partial T)_{\sigma_i}.$$

$$\Delta S_{LAT}^{PCE}(T, \sigma_i) = -V_m \int \left( \frac{\partial(\Delta a_i/a_i)}{\partial T} \right)_{\sigma_i} d\sigma_i \approx -V_m \cdot \alpha_{LAT}(T) \cdot \Delta \sigma_i. \quad (3)$$

The results of both procedures are shown in Fig. 3 for two external mechanical stresses, 0.05 and 0.1 GPa.

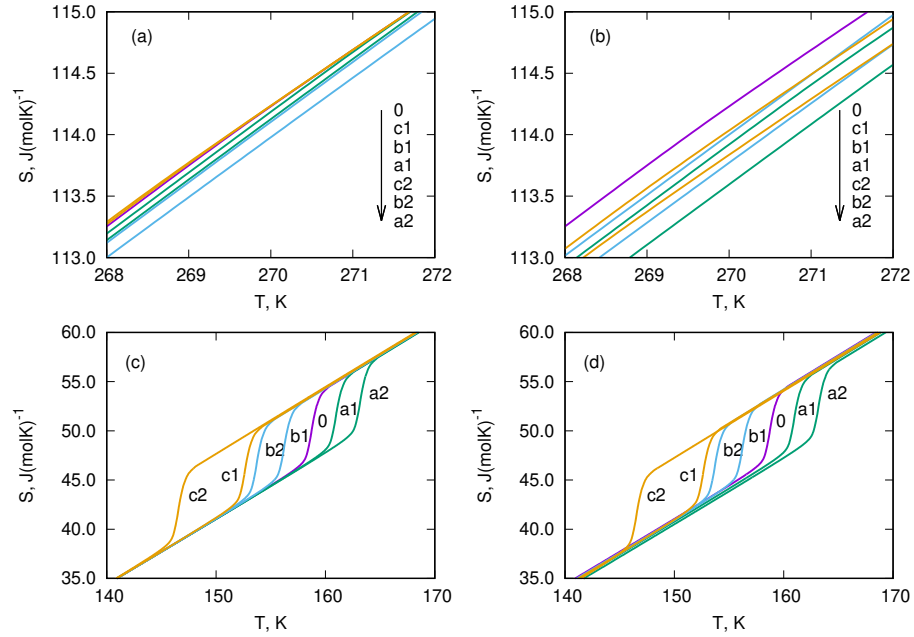


Figure 3: Temperature dependencies of total entropy of  $\text{NH}_4\text{HSO}_4$  at uniaxial stresses 0.05 (a1,b1,c1) and 0.1 GPa (a2,b2,c2) near (a,b)  $T_1$  and (c,d)  $T_2$  without taking into account (a,c) and taking into account (b,d) the thermal expansion of the crystal lattice.

When lattice expansion was not taken into account, the extensive PCE under stress along different axes was determined as a difference  $\Delta S_{PCE}(T, \sigma_i) = S(T, \sigma_i) - S(T, \sigma_i = 0)$  at constant temperature. The temperature dependencies of the intensive PCE were revealed analyzing plots of  $S(T, \sigma_i) = S_{LAT}(T, \sigma_i = 0) + \Delta S(T, \sigma_i)$  at constant entropy  $S(T, \sigma_i) = S(T + \Delta T_{AD}, \sigma_i = 0)$ . Fig. 4(a)-(d), 5(a)-(d) and 6(a)-(d) show the behavior of PCE associated with the main crystallographic axes in the region of both phase transitions. In accordance

with the sign of  $dT_1/d\sigma_i$  and  $dT_2/d\sigma_i$  (Table 1), PCE can be conventional and inverse.

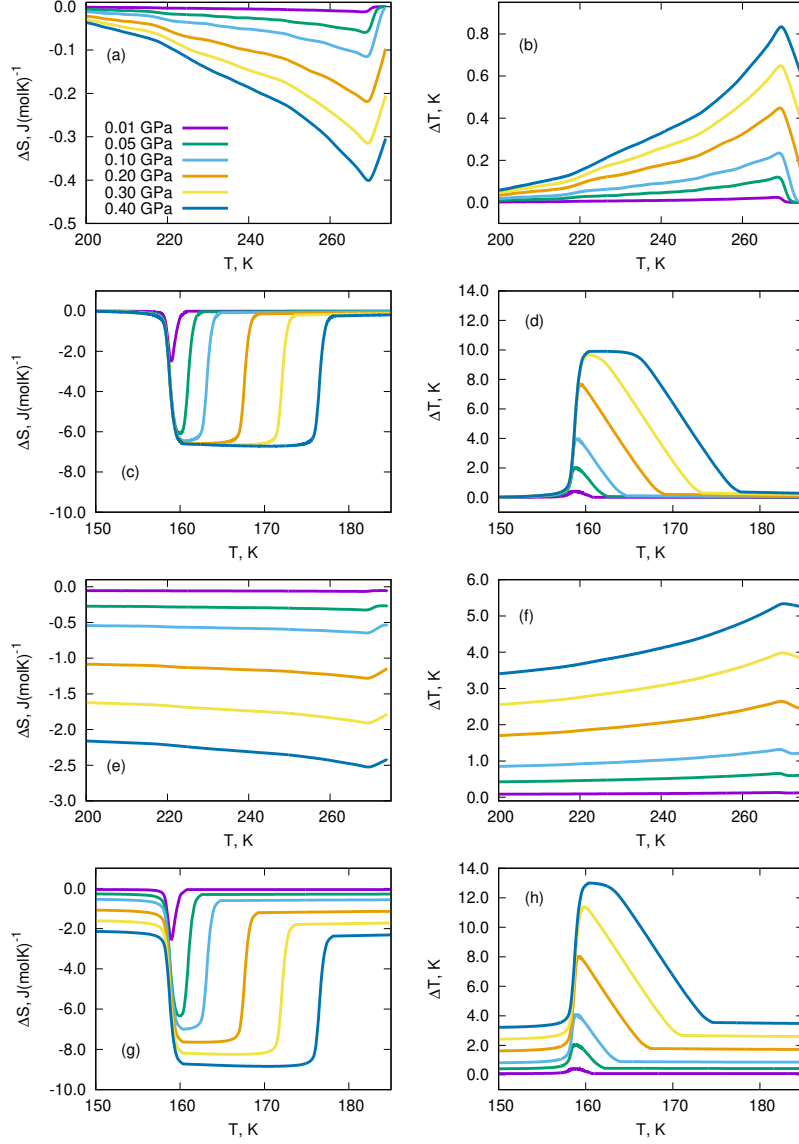


Figure 4: Piezocaloric entropy  $\Delta S_{PCE}$  and adiabatic temperature  $\Delta T_{AD}$  changes at different uniaxial stresses  $\sigma_a$  in temperature regions near  $T_1$  and  $T_2$  without taking into account (a,b,c,d) and taking into account (e,f,g,h) the thermal expansion of the crystal lattice.

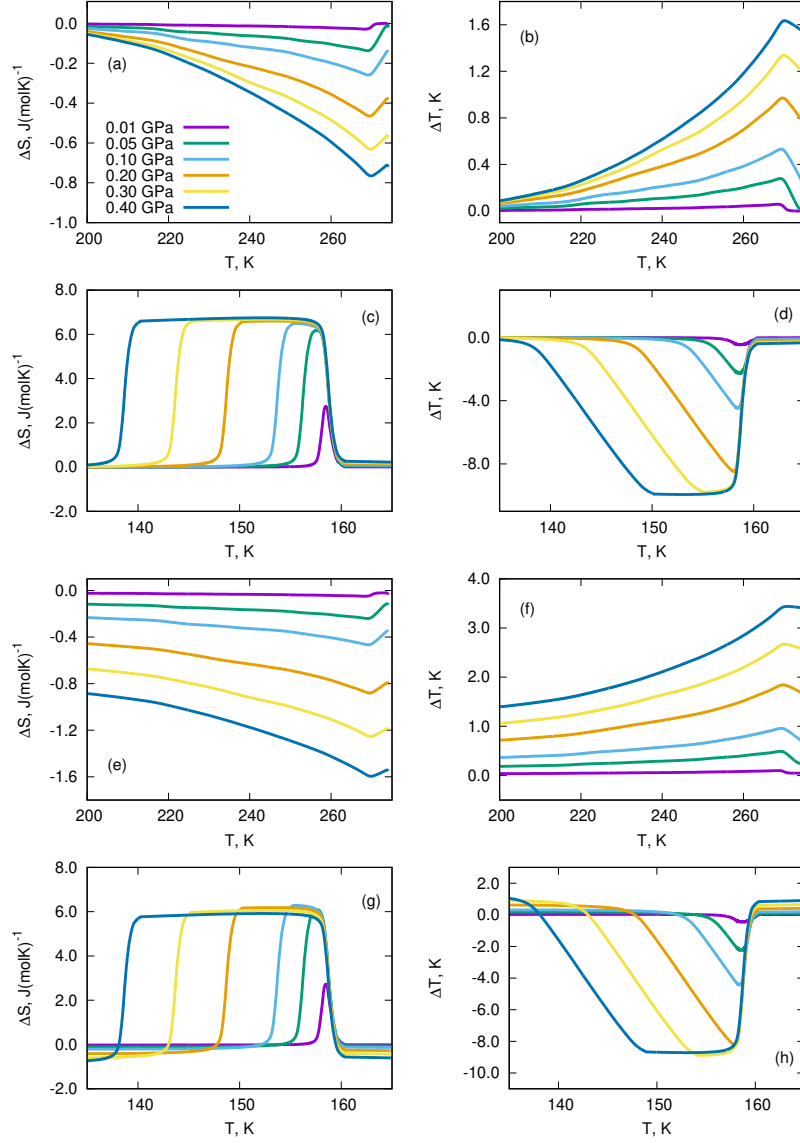


Figure 5: Piezocaloric entropy  $\Delta S_{PCE}$  and adiabatic temperature  $\Delta T_{AD}$  changes at different uniaxial stresses  $\sigma_b$  in temperature regions near  $T_1$  and  $T_2$  without taking into account (a,b,c,d) and taking into account (e,f,g,h) the thermal expansion of the crystal lattice.

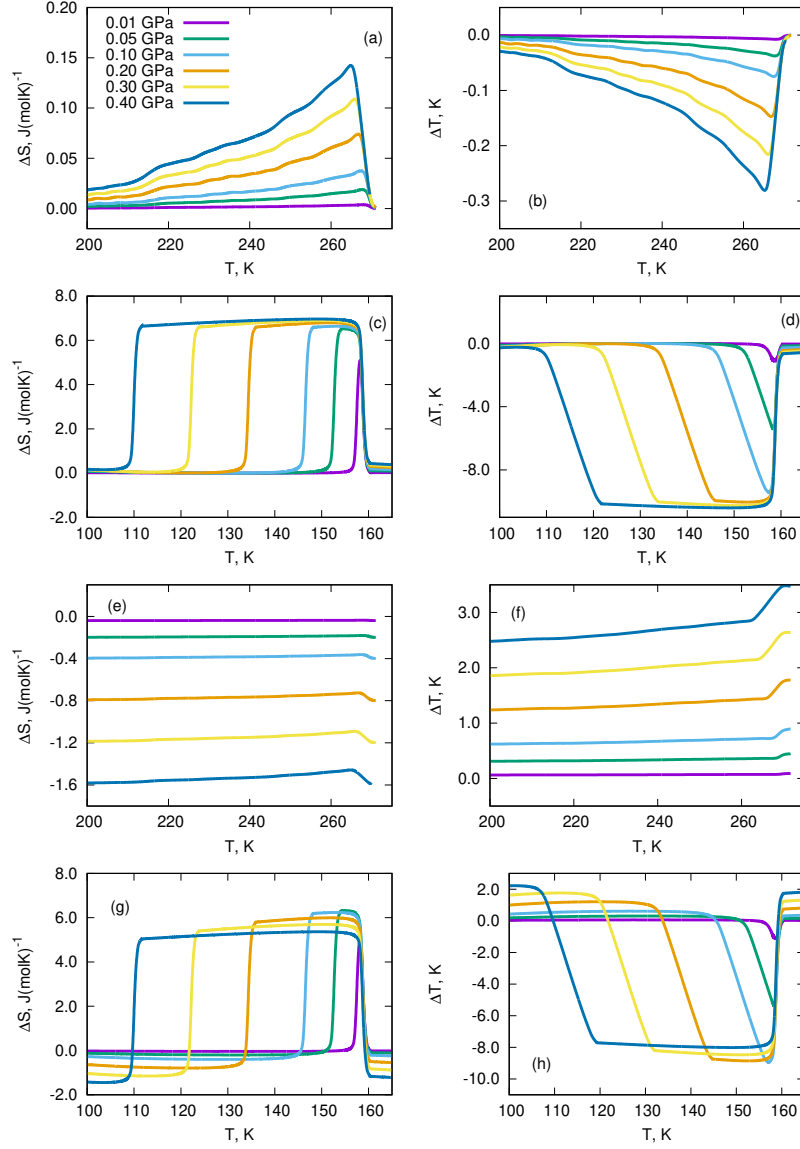


Figure 6: Piezocaloric entropy  $\Delta S_{PCE}$  and adiabatic temperature  $\Delta T_{AD}$  changes at different uniaxial stresses  $\sigma_c$  in temperature regions near  $T_1$  and  $T_2$  without taking into account (a,b,c,d) and with taking into account (e,f,g,h) the thermal expansion of the crystal lattice.



In the case of the phase transition at  $T_1$ , the maximum possible value of the extensive PCE equal to the entropy of the phase transition  $\Delta S_1=1.2$  J/mol·K has not been achieved even at  $\sigma_i=0.4$  GPa. Due to the most pronounced sensitivity of  $T_1$  to  $\sigma_b$  (Table 1),  $\text{NH}_4\text{HSO}_4$  shows at all pressures the largest values of PCE under stress along the  $b$  axis.

The values of the extensive PCE around  $T_2$  for all axes are rather close to the maximum value  $(\Delta S_{PCE})_{max} = \Delta S_2=6.7$  J/mol·K and can be realized at almost identical very low uniaxial pressures  $\approx 0.05$  GPa. However, to achieve the maximum magnitude of the intensive PCE,  $(\Delta T_{AD}^{\sigma_i})_{max} \approx 10$  K, significantly greater mechanical stresses are needed:  $\sigma_a \approx \sigma_b \approx 0.3$  GPa,  $\sigma_c \approx 0.1$  GPa. The slower saturation of  $\Delta T_{AD}$  under pressure is due to its strong dependence on two circumstances: first, on the derivative  $dS_{LAT}/dT$  and, second, on the baric coefficient  $dT/d\sigma$ .

Let us consider now the contribution of the lattice dilatation to the piezocaloric efficiency of  $\text{NH}_4\text{HSO}_4$ . Due to the positive sign of  $(\alpha_i)_{LAT}$  along all axes,  $\text{PCE}_{LAT}$  is always conventional. Fig. 3 (c), (d) show that the greatest decrease in  $S(T, \sigma_a)$  is associated with the largest magnitude of  $(\alpha_a)_{LAT}$ . At  $p=0.1$  GPa, the decrease in  $S(T, \sigma_i)$  is about 0.5% and 1% near  $T_1$  and  $T_2$ , respectively, and increases with pressure increase. As a result, extensive and intensive PCE undergo significant changes during both phase transitions.

At the transformation  $P2_1/c \leftrightarrow Pc$ , strong increase in both PCE was observed: at  $\sigma=0.4$  GPa, along all axes. The value  $\Delta S_{PCE}$  exceeds the entropy of the phase transition more than twice and  $\Delta T_{AD}$  also becomes very large ( $\approx 5$  K with  $\sigma_a$ ). One can also see that taking into account the lattice dilatation is accompanied by a change in PCE along the  $c$  axis from the inverse to the conventional (Fig. 6 (e), (f)).

Similar situation was observed at the phase transition  $Pc \leftrightarrow P1$ . Due to conventional origin of PCE associated with the positive sign of both  $\alpha_a$  and  $(\alpha_a)_{LAT}$ ,  $\text{NH}_4\text{HSO}_4$  shows the most pronounced increase in the extensive and intensive effects associated with the  $a$  axis: the maximum values are equal to  $\Delta S_{PCE}^a=-8.8$  J/mol·K and  $\Delta T_{AD}^a=13$  K at  $\sigma_a=0.4$  GPa (Fig. 4 (e), (g)). As

to PCE along axes  $b$  and  $c$ , different signs of  $\alpha_b < 0$ ,  $\alpha_c < 0$  and  $(\alpha_b)_{LAT} > 0$ ,  
 220  $(\alpha_c)_{LAT} > 0$  lead to decrease in both inverse effects and appearance of conven-  
 tional contributions that increase with increasing pressure more faster in compar-  
 ison with the decrease of inverse  $\Delta S_{PCE}$  and  $\Delta T_{AD}$  (Fig. 5, 6). It is neces-  
 sary to point out that the absolute values of the both total PCE,  $\sum |\Delta S_{PCE}^{b,c}| =$   
 $|\Delta S_{PCE}^{b,c}|_{inv} + |\Delta S_{PCE}^{b,c}|_{conv}$  and  $\sum |\Delta T_{AD}^{b,c}| = |\Delta T_{AD}^{b,c}|_{inv} + |\Delta T_{AD}^{b,c}|_{conv}$ ,  
 225 exceed the values observed without taking into account the lattice contribution  
 (Fig. 5, 6).

It is interesting to consider the relation between the dependences of  $\Delta S_{PCE}^{max}(\sigma_i)$   
 and  $\Delta T_{AD}^{max}(\sigma_i)$  for all axes at both phase transitions without and with taking  
 into account the expansion of the crystal lattice. At  $T_1$ , the behaviour of both  
 230 maximum effects is close to the linear (Fig. 7). However, it is necessary to be  
 cautious about this situation, as we suggested that the uniaxial pressure used  
 ( $\sigma \leq 0.4$  GPa) does not affect the magnitude of the coefficients  $\alpha$  and  $\alpha_{LAT}$ .

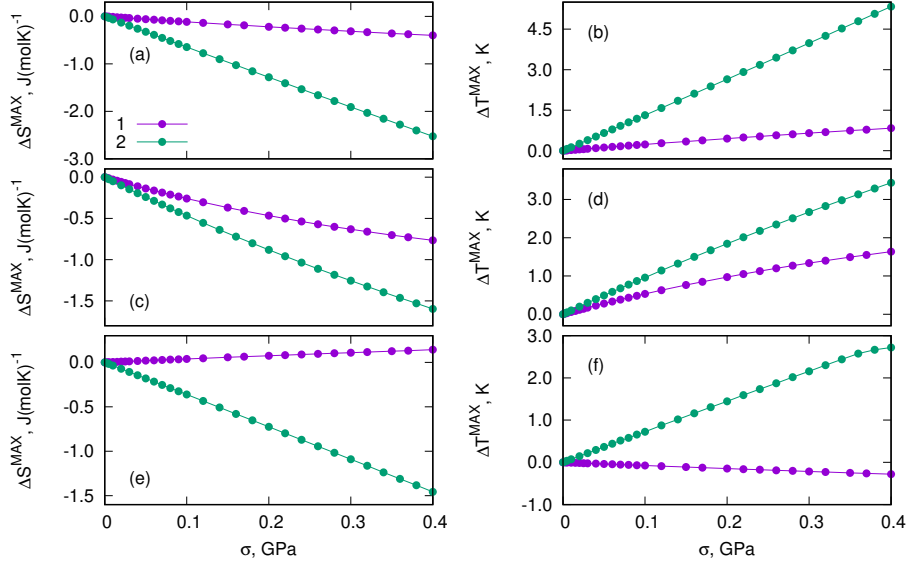


Figure 7: The dependencies of  $\Delta S_{PCE}^{max}$  and  $\Delta T_{AD}^{max}$  on uniaxial stresses along  $a$ -axis (a,b),  
 $b$ -axis (c,d) and  $c$ -axis (e,f) near  $T_1$  without (1) and with (2) taking into account the expansion  
 of the crystal lattice.

Fig. 8 clearly demonstrates that at  $T_2$ , the maximum values of  $\Delta S_{PCE}$  associated with each axis are realized at almost the same pressure. As to the values  $\Delta T_{AD}^{max}$ , they can be achieved at rather different uniaxial pressure for different axes in accordance with a large difference in baric coefficients  $dT/d\sigma_i$ . In Fig. 8, the dependencies  $\Delta S_{PCE}^{max}(\sigma_i)$  and  $\Delta T_{AD}^{max}(\sigma_i)$  for  $b$  and  $c$  axes with taking into account the lattice contribution are shown only for the part of inverse PCE. This is the reason why both maximum values decrease with increasing pressure.

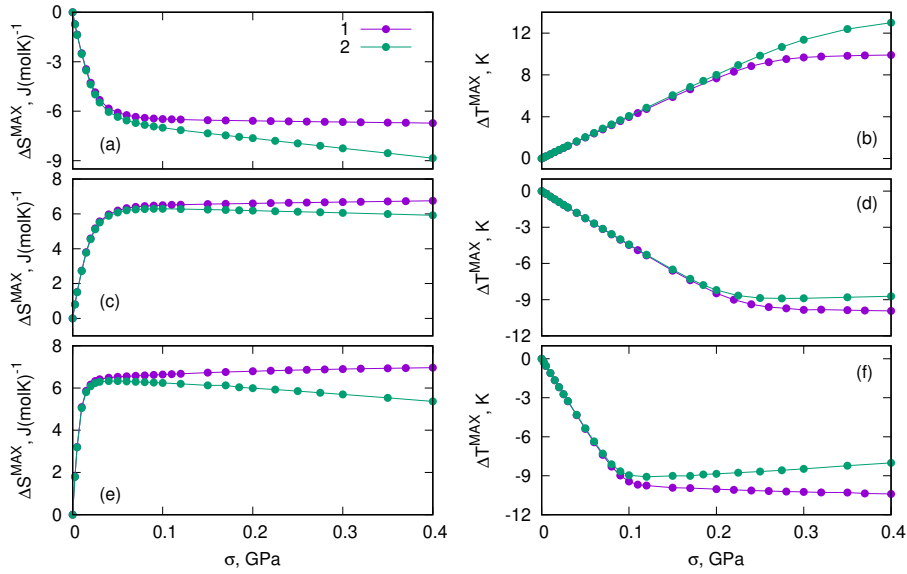


Figure 8: The dependencies of  $\Delta S_{PCE}^{max}$  and  $\Delta T_{AD}^{max}$  on uniaxial stresses along  $a$ -axis (a,b),  $b$ -axis (c,d) and  $c$ -axis (e,f) near  $T_2$  without (1) and with (2) taking into account the expansion of the crystal lattice.

The data on PCE in  $\text{NH}_4\text{HSO}_4$  are summarized in Table 2 in comparison with PCE in some other materials of the different origin.

One can see that the absolute maximum values of extensive and intensive effects are characteristic for different materials and can be realized with different mechanical stress  $\sigma$ . Very large value of  $\Delta S_{PCE}^{max}$  in ferroelastic  $(\text{NH}_4)_2\text{NbO}_2\text{F}_4$  observed under 0.9 GPa is a sum of two extensive effects associated with two temperature-close phase transitions [17]. When the uniaxial pressure decreases

Table 2: Piezocaloric characteristics at phase transitions in materials of different physical origin.

	Sample	$\Delta S_{PCE}^{max}$ , J/kg·K	$\sigma_i^{min}$ , GPa	$\Delta T_{AD}^{max}$ , K	$\sigma_i^{min}$ , GPa	Ref.
$\text{Cu}_{68}\text{Zn}_{16}\text{Al}_{16}$	Polycr.			6–7	0.275	[28]
$\text{Ni}_{48.9}\text{Ti}_{51.1}$	Wire	46	0.8	25	0.8	[29]
$\text{Ni}_{35}\text{Co}_{15}\text{Mn}_{35}\text{Ti}_{15}$	Polycr.			9.0	0.6	[12]
$\text{Ni}_{50}\text{Fe}_{19}\text{Ga}_{27}\text{Co}_4$	Single cr.	15	0.3	10	0.3	[30]
$\text{PbTiO}_3$	Calculated			13	0.5	[20]
$\text{PbTiO}_3$	Calculated			20	0.8	[31]
$\text{BaTiO}_3$	Thin film			4.6	6	[18]
$(\text{NH}_4)_2\text{NbOF}_5$	Single cr.					[17]
<i>c</i> -axis		110	0.9	-16	0.9	
<i>c</i> -axis		-50	0.3	-7	0.3	
$\text{NH}_4\text{HSO}_4$ (at $T_2$ )	Single cr.					This work
<i>a</i> -axis		-57	0.10	+10.0	0.30	
<i>b</i> -axis		+57	0.10	-10.0	0.30	
<i>c</i> -axis		+57	0.05	-10.0	0.10	

to the magnitude characteristic of PCE in  $\text{NH}_4\text{HSO}_4$  at  $T_2$ ,  $\sigma=0.1-0.3$  GPa, extensive effects in both materials become commensurate with each other. Large intense effect in a number of other materials was also observed under rather high  
 250 pressure (Table 2).

Thus, due to the low pressure necessary for the realization of  $\Delta S_{PCE}^{max}$  and  $\Delta T_{AD}^{max}$ , ammonium hydrogen sulphate can be considered as a rather efficient solid-state coolant. Moreover, strong anisotropy of PCE allows the sample of  $\text{NH}_4\text{HSO}_4$  to be heated or cooled by applying uniaxial pressure along different  
 255 directions. Obviously this feature can be used to design a hypothetical combined refrigeration cycle built on alternate application of pressure along different crystallographic axes. In the case of the phase transition at  $T_2$  in  $\text{NH}_4\text{HSO}_4$ , the combination of PCE associated with axes  $a$  and  $c$  looks the most promising.

Fig. 9 shows how a combined cycle can be organized. At the first stage,  
 260 applying uniaxial pressure along the  $a$  axis in adiabatic process 1 – 2 leads to increase in temperature. During the process 2 – 3' ( $\sigma_a = const$ ) heat transfers out from the refrigerant. Removal of  $\sigma_a$  (3 – 4,  $S = const$ ) is accompanied by the decrease in temperature. Further cooling (4 – 5,  $S = const$ ) is a result of applying pressure along the  $c$  axis,  $\sigma_c$ . In the process 5 – 6' ( $\sigma_c = const$ ), heat  
 265 transferred from the cooled reservoir to the refrigerant. Removal of  $\sigma_c$  (6' – 1,  $S = const$ ) causes the system to return to initial state.

It is obvious that at the same entropy change in individual and combined cycles, the efficiency of the latter cycle is much higher due to a significant expansion of the working temperature range. Moreover, in this case the filling  
 270 factor of the Carnot cycle 1-2-3-4-5-6-1 increases (Fig. 9).

Considered hypothetical cycle is also more convenient in comparison with the cycle based on a combination of two CE of different nature, ECE and PCE, recently analyzed [20]. One of the main reasons is that ECE is always accompanied by irreversible heating of the sample due to the release of Joule heat.

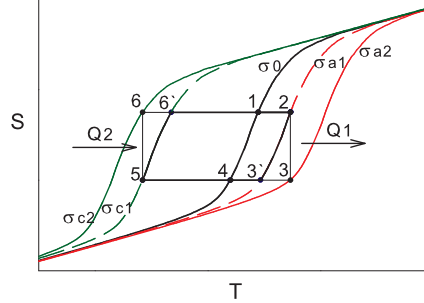


Figure 9: Hypothetical cooling cycle 1-2-3'-4-5-6'-1 built on the combination of the piezocaloric effect associated with axes  $a$  and  $c$ . 1-3-4-5-6-1 cycle is the Carnot cycle with the same changes of entropy.

#### 275 4. Conclusions

For the first time the effect of the anisotropy on caloric properties in ferroelectric material was studied.

Ammonium hydrogen sulphate undergoing a succession of two phase transitions was chosen as model object due to large difference in origin, type and  
280 sensitivity to external pressure of structural transformations.

Dilatometric and X-ray measurements revealed a strong anisotropy of thermal expansion in the region of both phase transitions which led to a significant difference in the signs and values of linear baric coefficients and as a result to anisotropy in piezocaloric properties. The greatest magnitudes of PCE at  $T_1$   
285 and  $T_2$  are related to different axes and provide the main contribution to the barocaloric effect, considered as the sum of linear effects. The pressure behaviour of the intensive and extensive PCE at the  $P2_1/c \leftrightarrow Pc$  phase transition is close to the linear and as a result both of them do not show saturation even at  $\sigma \approx 0.4$  GPa. At the same time, a strong nonlinearity of the dependences  
290  $\Delta S_{PCE}(\sigma_i)$  and  $\Delta T_{AD}(\sigma_i)$  at the first order transformation  $Pc \leftrightarrow P1$  is established, leading to low mechanical stresses to achieve the maximum possible values of PCE.  $\Delta S_{PCE}^{max} - \sigma_i = 0.05 - 0.10$  GPa and  $\Delta T_{AD}^{max} - \sigma_i = 0.10 - 0.30$  GPa.

Taking into account the thermal expansion of the crystal lattice, which was found to be positive in all directions, led to the greatest changes in PCE at  $T_1$ .  
295 The extensive effect equal to the entropy of the phase transition was achieved under rather low uniaxial pressure of 0.25 – 0.30 GPa.

At  $T_2$ , the  $\Delta S_{PCE}$  and  $\Delta T_{AD}$  magnitudes associated with axis  $a$  and showing a conventional PCE increased by about 30% at  $\sigma_a=0.4$  GPa. Due to inverse PCE along  $b$  and  $c$  axes, these values were decreased. However, the absolute  
300 magnitudes,  $\sum |\Delta S_{PCE}^{b,c}| = |(\Delta S_{PCE}^{b,c})_{inv}| + |(\Delta S_{PCE}^{b,c})_{conv}|$  and  $\sum |\Delta T_{AD}^{b,c}| = |(\Delta T_{AD}^{b,c})_{inv}| + |(\Delta T_{AD}^{b,c})_{conv}|$ , exceed the values observed without taking into account the lattice contribution.

Comparison of PCE in materials of different physical origin shows that  $\text{NH}_4\text{HSO}_4$  can be considered as competitive solid refrigerant. Due to strong  
305 anisotropy of PCE, thermodynamic efficiency of the cooling cycle can be improved by alternate using uniaxial pressure along axes  $a$  and  $c$ .

## References

- [1] Y. V. Sinyavskii, Electrocaloric refrigerators: A promising alternative to current low-temperature apparatus, Chemical and Petroleum Engineering  
310 31 (1995) 295–306. doi:10.1007/BF01148217.
- [2] A. M. Tishin, Y. I. Spichkin, The Magnetocaloric Effect and its Applications, Institute of Physics Publishing, Bristol, United Kingdom, 2003.
- [3] K. A. Gschneidner Jr, V. K. Pecharsky, A. O. Tsokol, Recent developments in magnetocaloric materials, Reports on Progress in Physics 68 (2005)  
315 1479–1539. doi:10.1088/0034-4885/68/6/r04.
- [4] S. Kar-Narayan, N. D. Mathur, Direct and indirect electrocaloric measurements using multilayer capacitors, J. Phys. D: Appl. Phys. 43 (2010) 032002. doi:10.1088/0022-3727/43/3/032002.
- [5] X. Moya, N. D. Kar-Narayan, S. and Mathur, Caloric materials near ferroic  
320 phase transitions, Nature Materials 13 (2014) 439. doi:10.1038/nmat3951.

- [6] A. Smith, C. R. Bahl, R. Bjrk, K. Engelbrecht, K. K. Nielsen, N. Pryds, Materials challenges for high performance magnetocaloric refrigeration devices, *Advanced Energy Materials* 2 (2012) 1288–1318. doi:10.1002/aenm.201200167.
- 325 [7] P. Lloveras, A. Aznar, M. Barrio, P. Negrier, C. Popescu, A. Planes, L. Mañosa, E. Stern-Taulats, A. Avramenko, N. D. Mathur, X. Moya, J.-L. Tamarit, Colossal barocaloric effects near room temperature in plastic crystals of neopentylglycol, *Nature Commun.* 10 (2019) 1803. doi:10.1038/s41467-019-09730-9.
- 330 [8] M. Valant, Electrocaloric materials for future solid-state refrigeration technologies, *Progress in Materials Science* 57 (2012) 980–1009. doi:10.1016/j.pmatsci.2012.02.001.
- [9] J. P. Joule, On some thermo-dynamic properties of solids, *Phil. Trans.* 149 (1859) 91–131.
- 335 [10] D. Soto-Parra, E. Vives, L. Mañosa, J. A. Matutes-Aquino, H. Flores-Zúñiga, A. Planes, Elastocaloric effect in Ti–Ni shape-memory wires associated with the  $B_2 - B_{19}'$  and  $B_2 - R$  structural transitions, *Appl. Phys. Lett.* 108 (2016) 071902. doi:10.1063/1.4942009.
- [11] C. Bechtold, C. Chluba, R. Lima de Miranda, E. Quandt, High cyclic stability of the elastocaloric effect in sputtered TiNiCu shape memory films, *Appl. Phys. Lett.* 101 (9) (2012) 091903. doi:10.1063/1.4748307.
- 340 [12] Z. Y. Wei, W. Sun, Q. Shen, Y. Shen, Y. F. Zhang, E. K. Liu, J. Liu, Elastocaloric effect of all-d-metal heusler NiMnTi(Co) magnetic shape memory alloys by digital image correlation and infrared thermography, *Appl. Phys. Lett.* 114 (2019) 101903. doi:10.1063/1.5077076.
- 345 [13] H. Sehitoglu, Y. Wu, E. Ertekin, Elastocaloric effects in the extreme, *Scripta Materialia* 148 (2018) 122–126. doi:10.1016/j.scriptamat.2017.05.017.

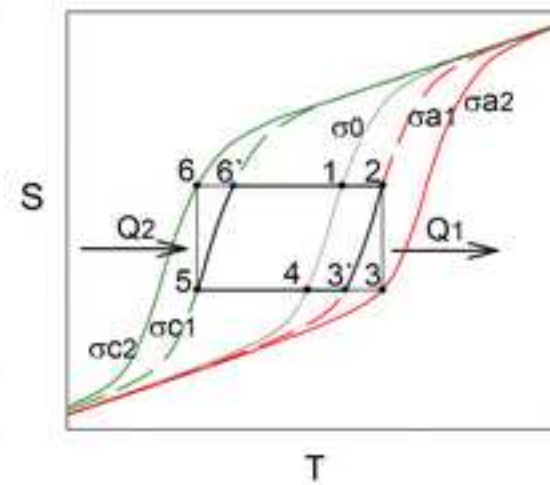
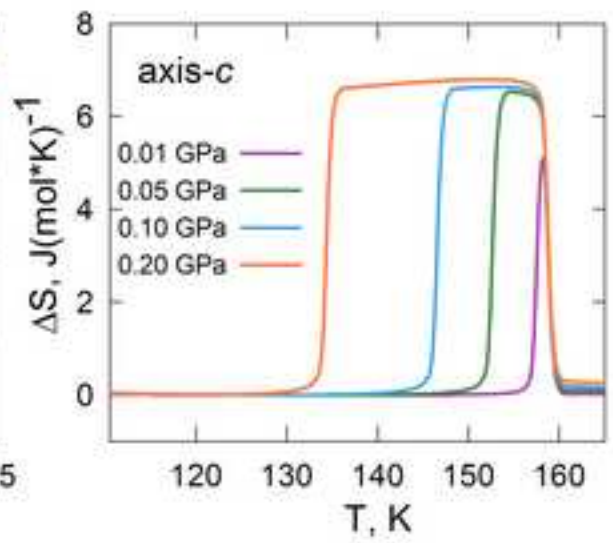
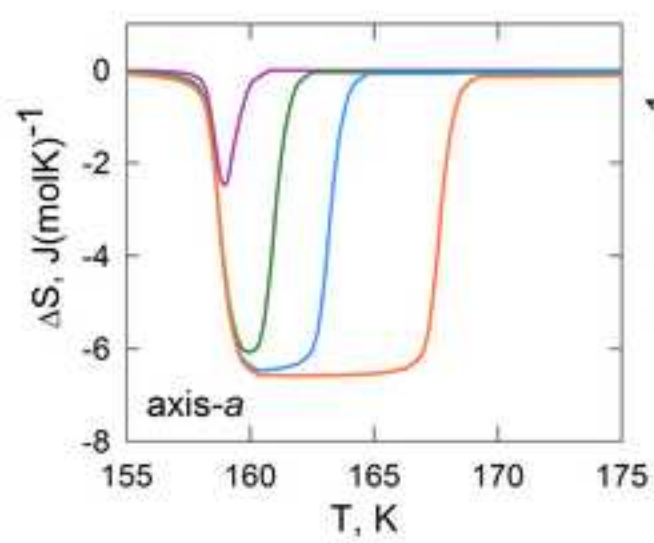


- [14] B. Lu, J. Liu, Mechanocaloric materials for solid-state cooling, *Science Bulletin* 60 (2015) 1638–1643. doi:10.1007/s11434-015-0898-5.
- [15] L. Mañosa, A. Planes, Materials with giant mechanocaloric effects: Cooling by strength, *Advanced Materials* 29 (2017) 1603607. doi:10.1002/adma.201603607.
- [16] M. Gorev, E. Bogdanov, I. Flerov, A. Kocharova, N. Laptash, Investigation of thermal expansion, phase diagrams, and barocaloric effect in the  $(\text{NH}_4)_2\text{WO}_2\text{F}_4$  and  $(\text{NH}_4)_2\text{MoO}_2\text{F}_4$  oxyfluorides, *Physics of the Solid State* 52 (2010) 167–175. doi:10.1134/S1063783410010294.
- [17] M. Gorev, E. Bogdanov, I. Flerov, N. Laptash, Thermal expansion, phase diagrams and barocaloric effects in  $(\text{NH}_4)_2\text{NbOF}_5$ , *Journal of Physics: Condensed Matter* 22 (2010) 185901. doi:0953-8984/22/i=18/a=185901.
- [18] Y. Liu, I. C. Infante, X. Lou, L. Bellaiche, J. F. Scott, B. Dkhil, Giant room-temperature elastocaloric effect in ferroelectric ultrathin films, *Advanced Materials* 26 (2014) 6132–6137. doi:10.1002/adma.201401935.
- [19] S. Patel, A. Chauhan, R. Vaish, Elastocaloric and piezocaloric effects in lead zirconate titanate ceramics, *Energy Technology* 4 (2016) 647–652. doi:10.1002/ente.201500446.
- [20] H. Khassaf, T. Patel, S. P. Alpay, Combined intrinsic elastocaloric and electrocaloric properties of ferroelectrics, *J. Appl. Phys.* 121 (2017) 144102. doi:10.1063/1.4980098.
- [21] G. Bai, Q. Xie, J. Xu, C. Gao, Large negative piezocaloric effect: Uniaxial stress effect, *Solid State Commun.* 291 (2019) 11–14. doi:10.1016/j.ssc.2019.01.002.
- [22] Energy savings potential and rd&d opportunities for non-vapor-compression hvac technologies, report of the u.s. dpt. of energy, march 2014.

- [23] E. Mikhaleva, I. Flerov, A. Kartashev, M. Gorev, E. Bogdanov, V. Bondarev, Thermal, dielectric and barocaloric properties of  $\text{NH}_4\text{HSO}_4$  crystallized from an aqueous solution and the melt, *Solid State Sciences* 67 (2017) 1–7. doi:10.1016/j.solidstatesciences.2017.03.004.
- 380 [24] P. Lloveras, E. Stern-Taulats, M. Barrio, J.-L. Tamarit, S. Crossley, W. Li, V. Pomjakushin, A. Planes, L. Mañosa, N. D. Mathur, X. Moya, Giant barocaloric effects at low pressure in ferroelectric ammonium sulphate, *Nature Communications* 6 (2015) 8801. doi:10.1038/ncomms9801.
- [25] R. Pepinsky, K. Vedam, S. Hoshino, Y. Okaya, Ammonium hydrogen sulfate: A new ferroelectric with low coercive field, *Phys. Rev.* 111 (1958) 1508–1510. doi:10.1103/PhysRev.111.1508.
- 385 [26] D. Swain, V. S. Bhadram, P. Chowdhury, C. Narayana, Raman and x-ray investigations of ferroelectric phase transition in  $\text{NH}_4\text{HSO}_4$ , *J. Phys. Chem. A* 116 (2012) 223–230. doi:10.1021/jp2075868.
- [27] A. V. Kartashev, I. N. Flerov, N. V. Volkov, K. A. Sablina, Adiabatic calorimetric study of the intense magnetocaloric effect and the heat capacity of  $(\text{La}_{0.4}\text{Eu}_{0.6})_{0.7}\text{Pb}_{0.3}\text{MnO}_3$ , *Phys. Solid State* 50 (2008) 2115–2120. doi:10.1134/S1063783408110188.
- 390 [28] L. Mañosa, S. Jarque-Farnos, E. Vives, A. Planes, Large temperature span and giant refrigerant capacity in elastocaloric Cu–Zn–Al shape memory alloys, *Appl. Phys. Lett.* 103 (2013) 211904. doi:10.1063/1.4832339.
- [29] J. Tušek, K. Engelbrecht, L. P. Mikkelsen, N. Pryds, Elastocaloric effect of Ni–Ti wire for application in a cooling device, *J. Appl. Phys.* 117 (2015) 124901. doi:10.1063/1.4913878.
- 400 [30] F. Xiao, M. Jin, J. Liu, X. Jin, Elastocaloric effect in  $\text{Ni}_{50}\text{Fe}_{19}\text{Ga}_{27}\text{Co}_4$  single crystals, *Acta Materialia* 96 (2015) 292–300. doi:10.1016/j.actamat.2015.05.054.

- [31] S. Lisenkov, B. K. Mani, C.-M. Chang, J. Almand, I. Ponomareva, Multicaloric effect in ferroelectric  $\text{PbTiO}_3$  from first principles, Phys. Rev. B 87 (2013) 224101. doi:10.1103/PhysRevB.87.224101.

405



- The effect of anisotropy on the piezocaloric properties of  $\text{NH}_4\text{HSO}_4$  are studied.
- A significant difference in signs and values of linear baric coefficients are found.
- 
- The greatest piezocaloric effects at  $\text{Pc} \leftrightarrow \text{P1}$  transition are realized at low pressure.
- 
- Crystal lattice expansion strongly affects the piezocaloric properties at  $T_1$ .
- 
- Effective cooling cycle is proposed by using uniaxial pressure along different axes

**LaTeX Source Files**

[Click here to download LaTeX Source Files: flerov\\_manuscript.zip](#)